Supporting Information

Fluorescence detection of phosphate in an aqueous environment by an aluminum-based metal-organic framework with amido ligands

Peng Li[a,b,*], Lingqian Dong[a,b], Jingren Yang[a], Yonghui Tu[a], Chao Wang[a,b], Yiliang He[a,b]

[a] *School of Environmental Science & Engineering, Shanghai Jiao Tong University, Shanghai, 200240, China.*

[b] *China-UK Low Carbon College, Shanghai Jiao Tong University, Shanghai, 200240, China.*

* Corresponding authors.

E-mail addresses: lipeng2016@sjtu.edu.cn (P. Li)

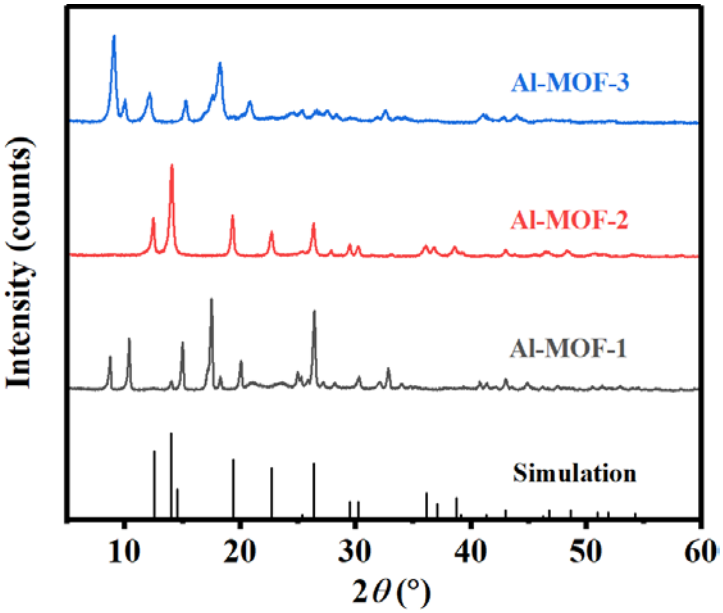

Figure S1. XRD patterns of Al-MOF-1, Al-MOF-2 and Al-MOF-3. (Al-MOF-1, Al-MOF-2, Al-MOF-3 were synthesized with deionized water, glacial acetic acid, and DMF as solvents respectively)

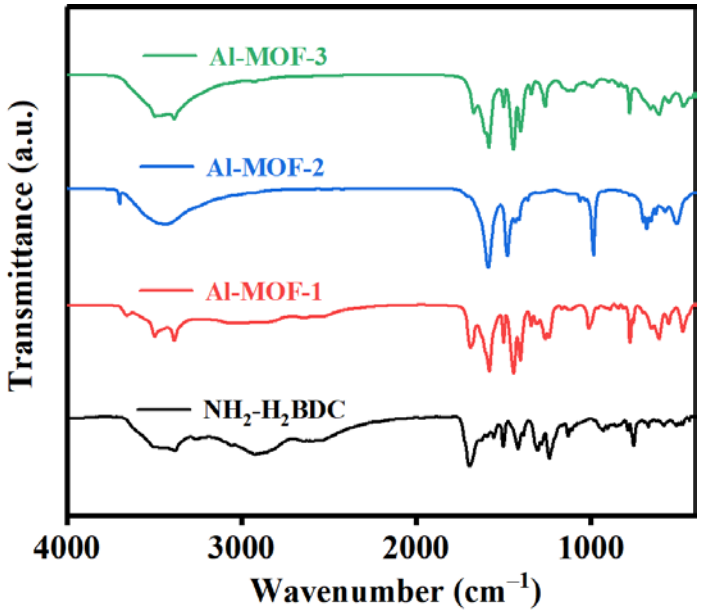

Figure S2. Comparison of FTIR spectra of NH_2-H_2BDC, Al-MOF-1, Al-MOF-2 and Al-MOF-3. (Al-MOF-1, Al-MOF-2, Al-MOF-3 were synthesized with deionized water, glacial acetic acid, and DMF as solvents respectively)

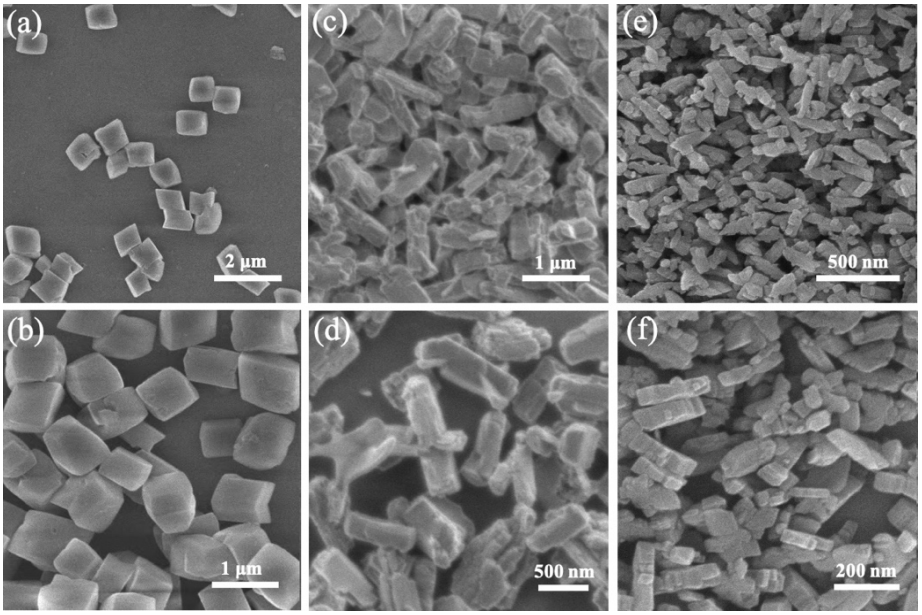

Figure S3. (a)(b) SEM images of Al-MOF-1; (c)(d) SEM images of Al-MOF-2; (e)(f) SEM images of Al-MOF-3. (Al-MOF-1, Al-MOF-2, Al-MOF-3 were synthesized with deionized water, glacial acetic acid, and DMF as solvents respectively)

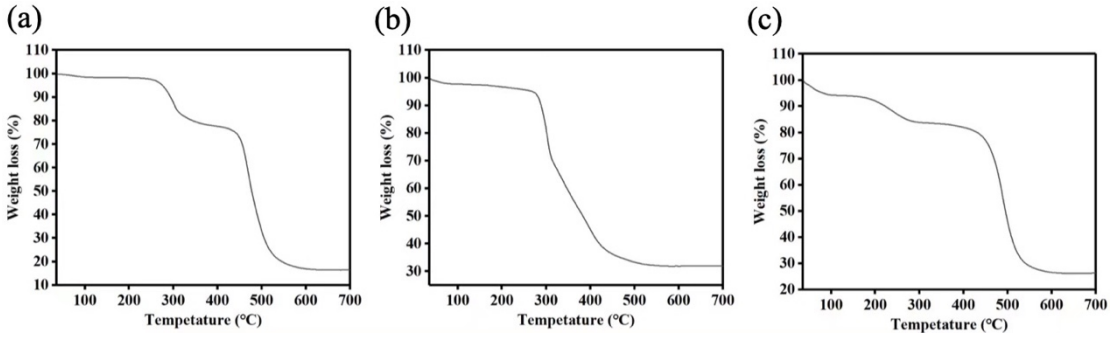

Figure S4. (a) TG curve of Al-MOF-1; (b) TG curve of Al-MOF-2; (c) TG curve of Al-MOF-3, which were recorded in an air atmosphere in the temperature range of 25-700 °C with a heating rate of 10 °C min^{-1}. (Al-MOF-1, Al-MOF-2, Al-MOF-3 were synthesized with deionized water, glacial acetic acid, and DMF as solvents respectively)

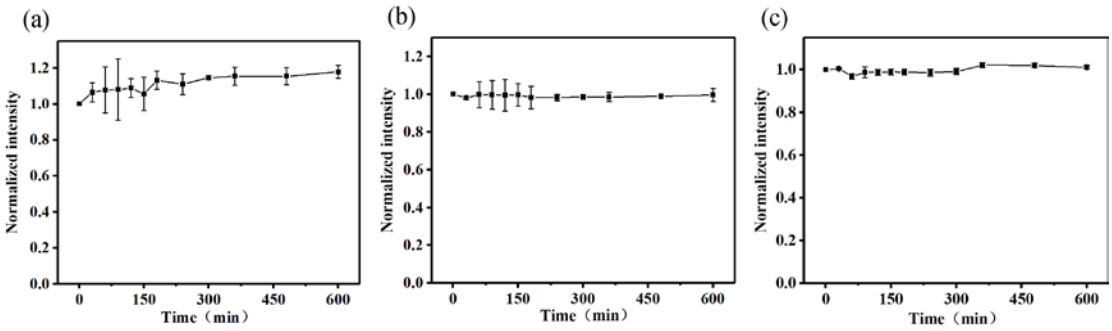

Figure S5. (a) The change in fluorescence intensity of Al-MOF-1 with different time; (b) the change in fluorescence intensity of Al-MOF-2 with different time; (c) the change in fluorescence intensity of Al-MOF-3 with different time. (Al-MOF-1, Al-MOF-2, Al-MOF-3 were synthesized with deionized water, glacial acetic acid, and DMF as solvents respectively)

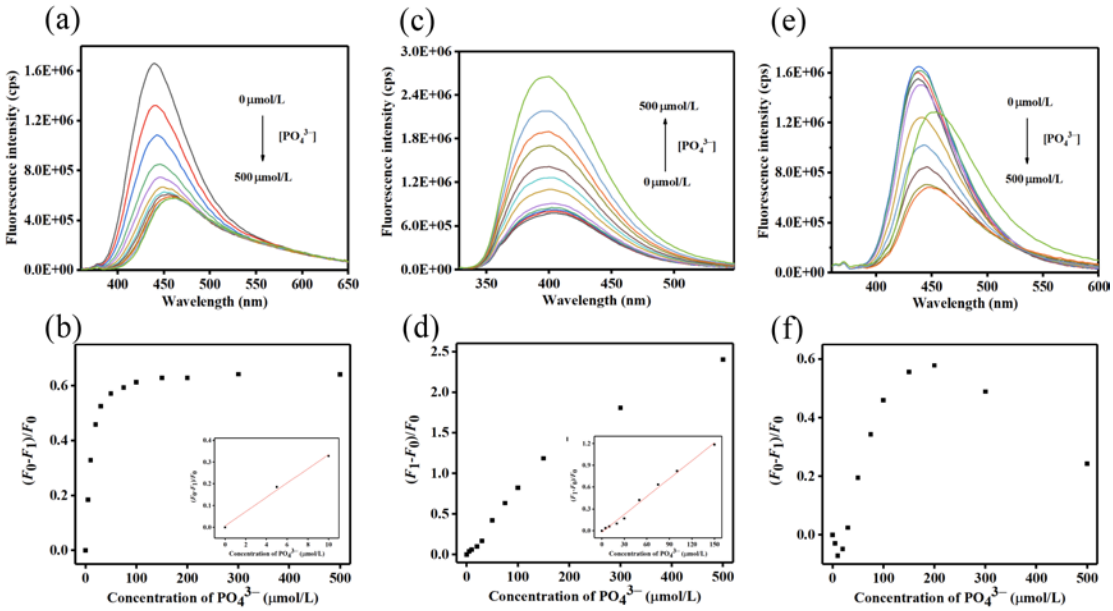

Figure S6. (a)(c)(e) Fluorescence emission spectra of Al-MOF-1, Al-MOF-2 and Al-MOF-3 in the presence of different concentrations of PO_4^{3-}. (b)(d)(f) the relationship between the fluorescence change efficiency of Al-MOF-1, Al-MOF-2 and Al-MOF-3 and phosphate concentration. (Al-MOF-1, Al-MOF-2, Al-MOF-3 were synthesized with deionized water, glacial acetic acid, and DMF as solvents respectively)

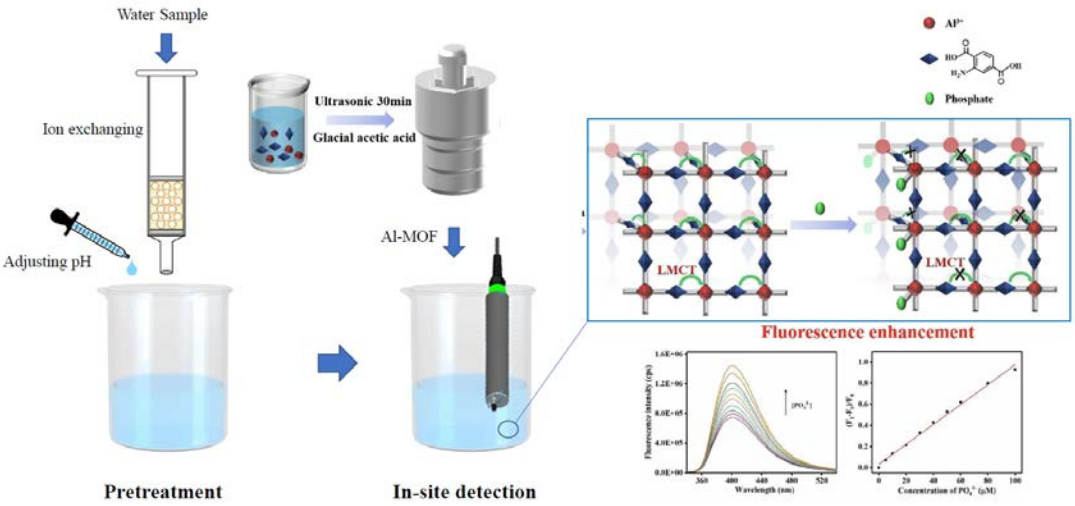

Fig. S7 the operation diagram of the on-site phosphate detection method

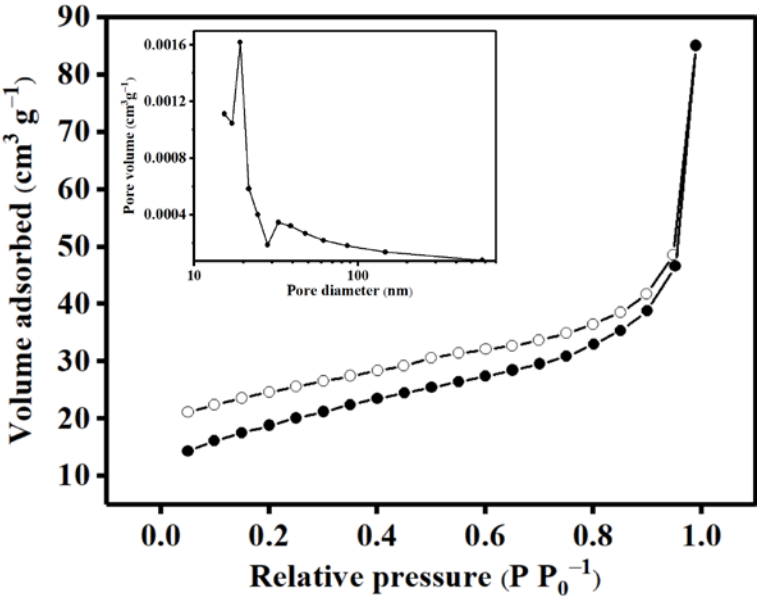

Figure S8. N_2 adsorption (solid circles) and desorption (empty circles) isotherms of Al-MOF and the corresponding pore size distribution (the inset).

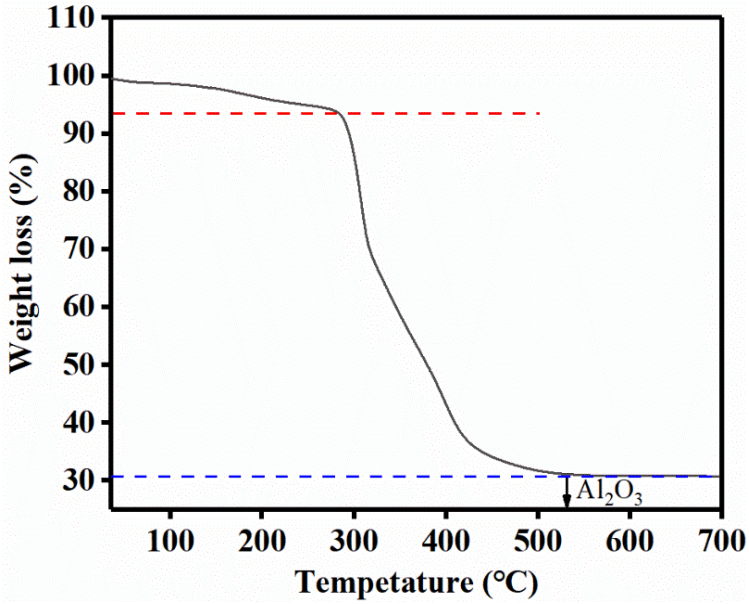

Figure S9. TG curves of the Al-MOF recorded in an air atmosphere in the temperature range of 25-700 °C with a heating rate of 10 °C min^{-1}.

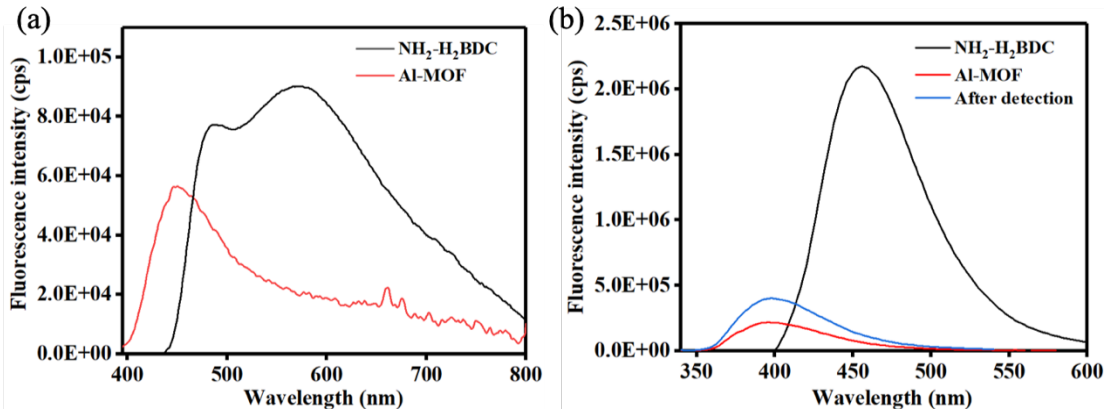

Figure S10. (a) Solid-state fluorescence spectra of free NH_2-H_2BDC ligand and Al-MOF; (b) fluorescence spectra of free NH_2-H_2BDC ligand, Al-MOF and Al-MOF after detection in the aqueous solutions.

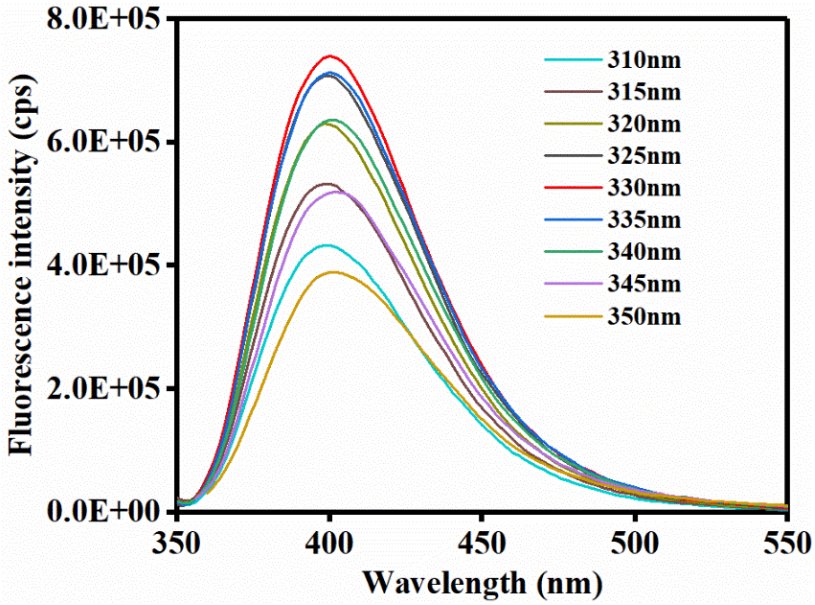

Figure S11. Fluorescence emission spectra of Al-MOF (100 mg L^{-1}) with the range of excitation wavelength from 310 nm to 350 nm.

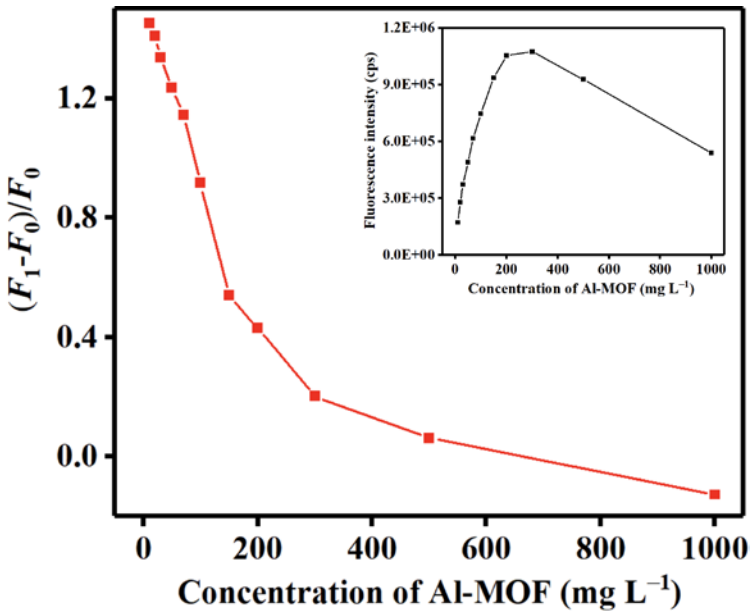

Figure S12. Fluorescence enhancement efficiency of Al-MOF with the concentrations of 0-1000 mg L^{-1} upon the addition of PO_4^{3-} (100 μM), the inset presents the fluorescence intensity of Al-MOF with concentration from 0 mg L^{-1} to 1000 mg L^{-1}.

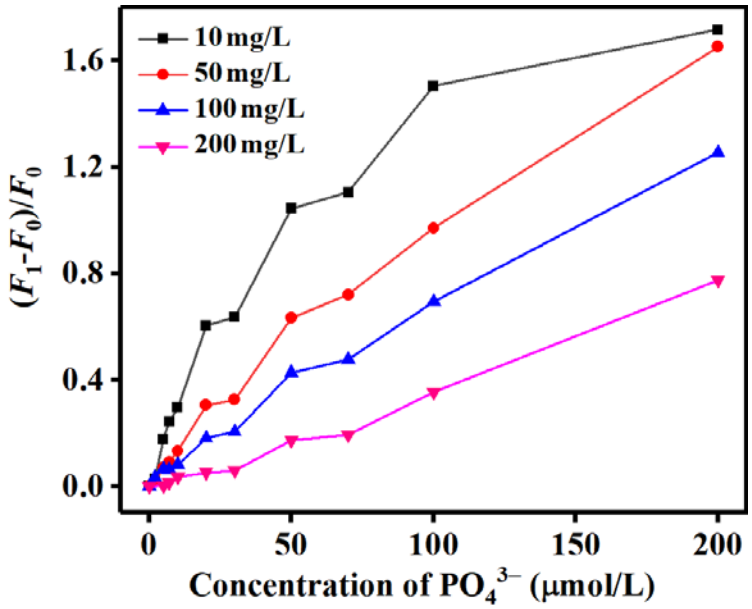

Figure S13. Fluorescence enhancement efficiency of Al-MOF (10 mg L^{-1}, 50 mg L^{-1}, 100 mg L^{-1}, 200 mg L^{-1}) with different concentrations of PO_4^{3-}. (F_0 and F_1 are the fluorescence intensities of Al-MOF (λ_{ex}=330 nm, λ_{em}=402 nm) in the absence and presence of PO_4^{3-}, respectively)

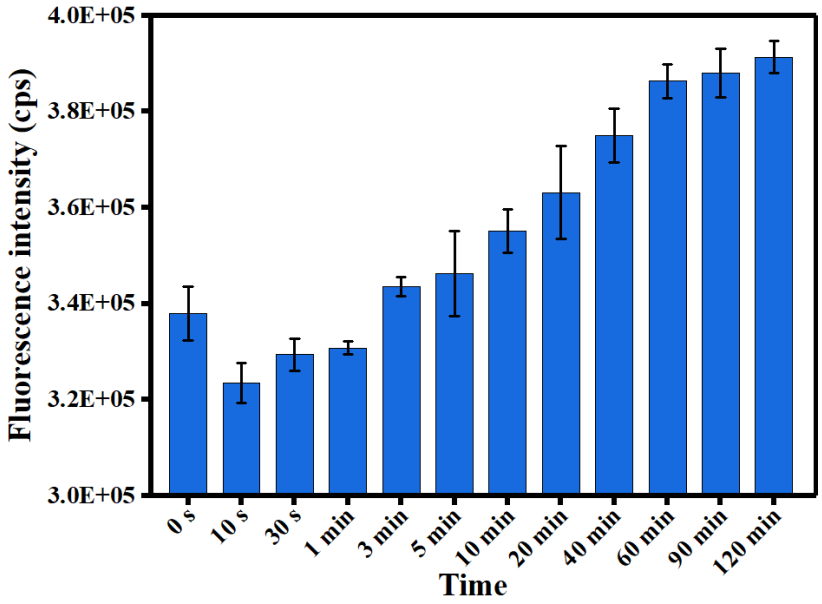

Figure S14. The fluorescence intensity of Al-MOF (20 mg L^{-1}) at λ_{em}=402 nm (λ_{ex}=330 nm) with different incubation time upon the addition of PO_4^{3-} (20 μM).

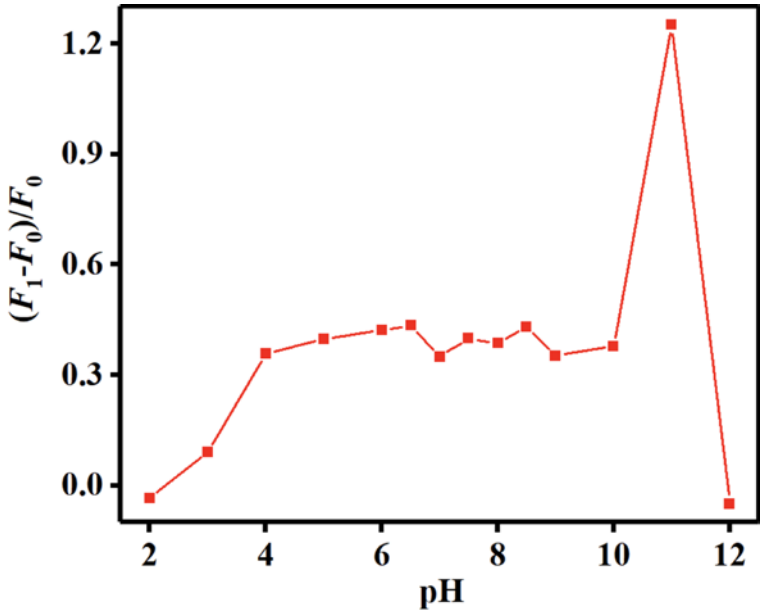

Figure S15. Fluorescence enhancement efficiency of Al-MOF with the solution pH of 2-12 upon the addition of PO_4^{3-} (100 μM), the inset presents the fluorescence intensity of Al-MOF with solution pH from 2 to 12. (F_0 and F_1 are the fluorescence intensities of Al-MOF (λ_{ex}=330 nm, λ_{em}=402 nm) in the absence and presence of PO_4^{3-}, respectively).

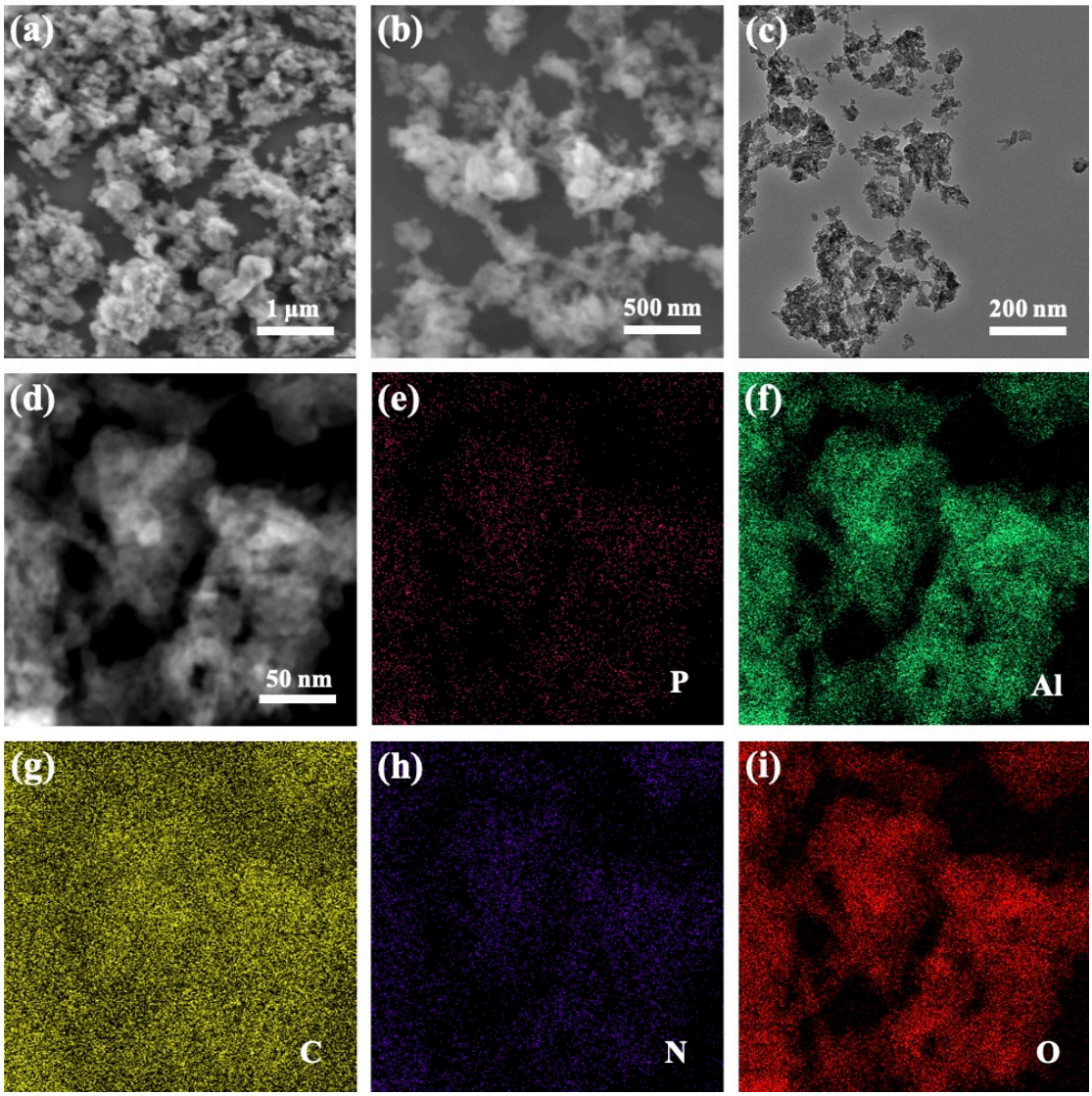

Figure S16. (a)(b) SEM images of Al-MOF after adsorption PO_4^{3-}; (c)(d) TEM images of Al-MOF after adsorption PO_4^{3-}; (e)-(i) element mapping for P, Al, C, N, O, respectively.

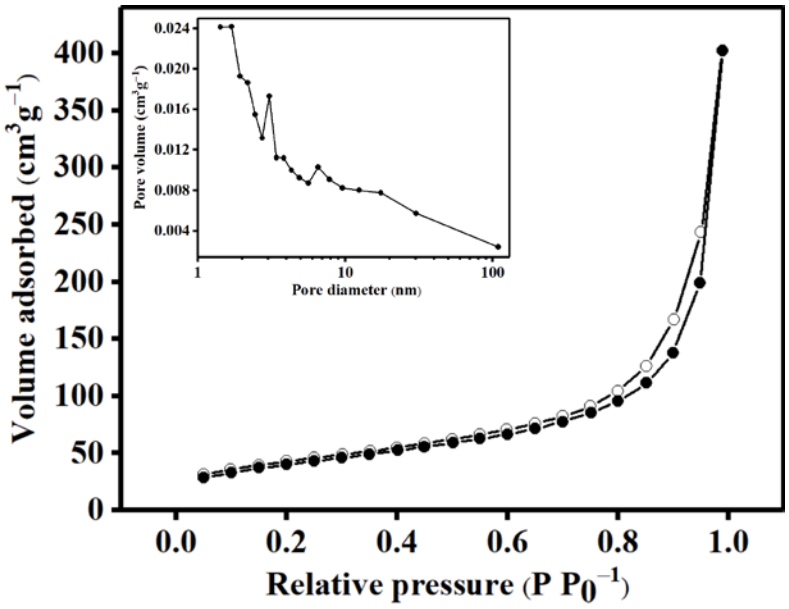

Figure S17. N_2 adsorption (solid circles) and desorption (empty circles) isotherms of Al-MOF after detection and the corresponding pore size distribution (the inset).

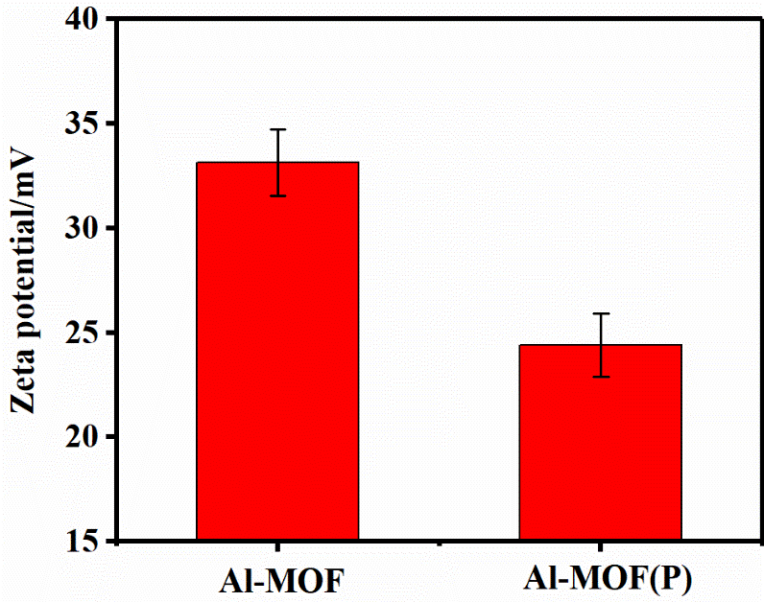

Figure S18. Zeta potential values of the Al-MOF and Al-MOF after detection.

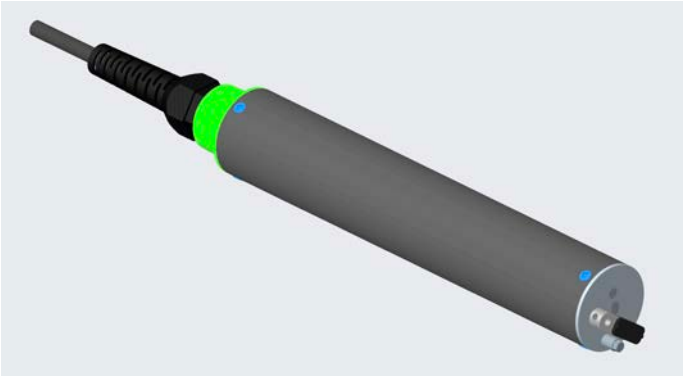

(a)

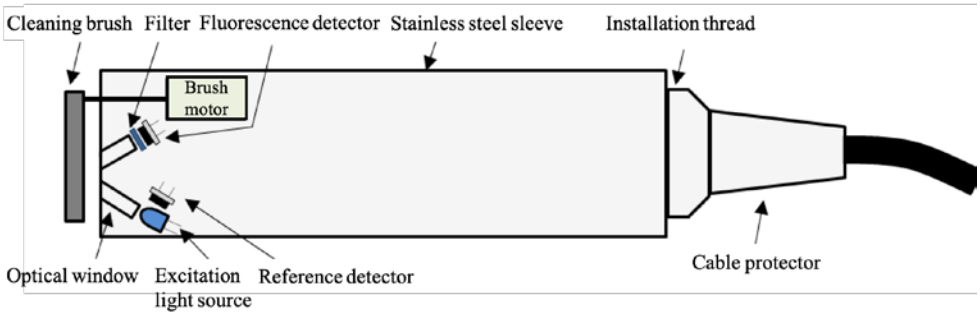

(b)

Figure S19. (a) The external of phosphate digital sensor; (b) the internal structure of phosphate digital sensor.

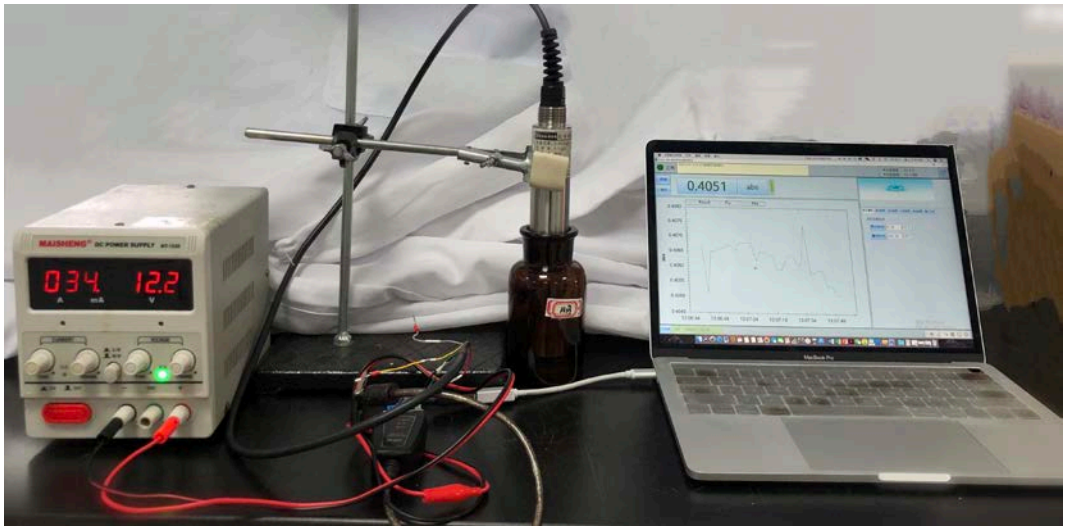

Figure S20. Phosphate online monitoring field test chart.